CONVERGENT FLOW AND SIMPLE AIR INTAKES WITH A LIMITING COMPACT CHANNEL

B. I. Gutov and V. V. Zatoloka

UDC 533.6.011

A consideration was made in [1] of convergent air intakes (CAI), which are so named because the transverse cross section of the layers flowing into the air intakes are compressed by its walls along intersecting lines, i.e., convergently. One can also call the compression flow in a CAI convergent. This special name was given to this type of air intake by E. S. Shchetinkov since he was the first to recognize its importance. They are distinguished by the compact nature of transverse cross sections of the channel and the spatial character of the flow in them.

We will consider a class of CAI [2-5] that was initially constructed of simple combinations of planar flows on the basis of the gas dynamic design method [6, 7]. We will then use a simple method (cutting along the surfaces of the flow) to construct a large variety of configurations, including a CAI with a limiting compact channel. The compact nature of the channel is the chief feature distinguishing the CAI from traditional widely known, and highly developed air intakes that are planar and circular with a central object but are divergent.

The initial compression surface for a simple CAI with planar walls and for a planar air intake (PAI) is the wedge 1 in Fig. 1. The compression face of this wedge forms the angle ϑ_1 with the direction of the incident flow, while the leading edge 2 of the wedge is perpendicular to it. The wedge with end faces is bounded by lateral cheeks 3 that are parallel to the direction of the incident flow for the PAI. However, the CAI has cheeks that are not parallel to one another but form an angle of φ_2 with one another. The longitudinal profiles for the PAI and CAI are equivalent (Fig. 1a), while the form differs from the front (b for the PAI and c for the CAI).

The initial discontinuity converging with the leading edge 2 [the Mach number of the incident flow is $M_I = M_{ID}$ (I is incident and ID is incident design), while the angle of attack is $\alpha = 0$] lies on the inclined leading edge 4 of the cheeks and is at an angle of ω_1 with the direction of the incident flow (for the CAI and the PAI). If the width of edge 5 for the PAI is equal to the width of the wedge (b), then it is equal to zero for the CAI (c). The inclined cheeks of the CAI generate secondary planar shock waves 6 with an angle of turn for the flow of ϑ_2 and an angle of inclination for the discontinuity relative to the incident flow of ω_2. These discontinuities also penetrate to the leading edge 4 of the cheeks and are perpendicular to the compression surface (face) of the wedge. This configuration for the external compression section 7 of the CAI is expressed by the following relations

$$\tan\vartheta_2 = \tan\omega_2/[1 + \tan(\omega_1 - \vartheta_1)/\tan\vartheta_1],$$
$$\tan(\varphi_2/2) = \tan\vartheta_2/\sin\vartheta_1.$$

The compression streams on the external compression section are achieved consecutively in two shock waves (a primary and secondary discontinuity), whose flow parameters are determined with known relations on shock waves.

Gas dynamic and geometric characteristics of these compression flows and of the CAI are determined by assigning two independent parameters such as M_{ID} and ϑ_1. The range over which these flows may exist (Fig. 2) is bounded by the curve AB and the axis for M_{ID}. Each point in this region has two solutions, one of which corresponds to a weak and the other of which corresponds to a strong secondary discontinuity intensity [2, 3]. The value of M is subsonic beyond the secondary discontinuity in the region ACDA for the second solution.

The degree of external compression of the transverse cross section of the captured stream for the simplified CAI (Fig. 1) is determined by the expression

$$\bar{F}_{input} = F_{ID}/F_{input} = \sin\omega_1 \cdot \sin\omega_2 \cdot \cos\vartheta_2/\sin(\omega_1 - \vartheta_1)\cdot\sin(\omega_2 - \vartheta_2), \quad (1)$$

Novosibirsk. Translated from Zhurnal Prikladnoi Mekhaniki i Tekhnicheskoi Fiziki, No. 2, pp. 57-62, March-April, 1987. Original article submitted February 12, 1986.

 0021-8944/87/2802-0216$12.50

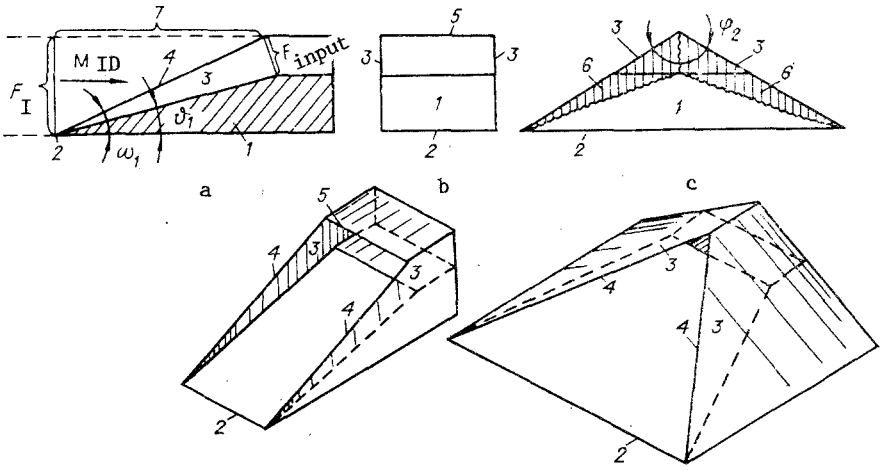

Fig. 1

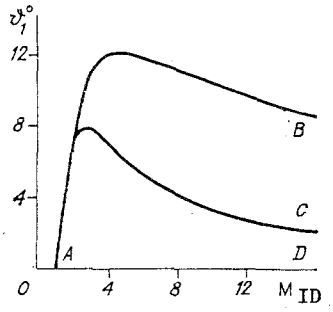

Fig. 2

where F_{ID} is the area of the captured stream cross section in the incident flow; F_{input} is the area of the stream in the cross section of the input to the channel, which passes through the point at which the edges of the lateral cheeks converge.

A principal feature distinguishing a CAI from a PAI is the convergent spatial nature of compression. Hence, the transverse cross sections of the captured stream in the incident flow and the channel are similar and have the form of a triangle for a simplified CAI, while for a PAI the stream is compressed in a single direction, and the cross section at the input to the channel is "flattened" in comparison with the cross section of the captured stream in the incident flow.

For supersonic air intakes, as compact a transverse channel cross section as possible is desirable, since its walls must have the smallest area and they must withstand extremely high thermal loading. One can use the coefficient k as a measure of compactness, where the perimeter of a given cross section P is many times greater than the length of the circumference of a circle with an area equal to the area of this cross section F. It is evident that

$$k = P/2\sqrt{\pi F},\ k \geqslant 1. \tag{2}$$

One can use the following equations for determining k for a triangular channel (for a simplified CAI, see Fig. 1)

$$k = [1 + \operatorname{cosec}(\varphi_2/2)]\sqrt{[\tan(\varphi_2/2)]/\pi}.$$

In the practical range of ϑ_1 = 5-10°, the angle φ_2 = 100-120°, while k = 1.4-1.6, i.e., it is noticeably greater than unity. With sharp angles for the transverse channel cross sections, there will be undesirable interference of the boundary layers (see Fig. 1c).

By sectioning of convergent cross sections along the flow surface with successive substitution of their solid walls, one can construct many different new air intakes whose channel inputs (and external compression sections) are more compact with transverse cross section angles close to or greater than 90°.

We will consider a sectioning (Fig. 3a) of the captured stream transverse cross section into a symmetric rectangle, where one of the angles coincides with φ_2 and the other $\varphi_1 \leq 180°$

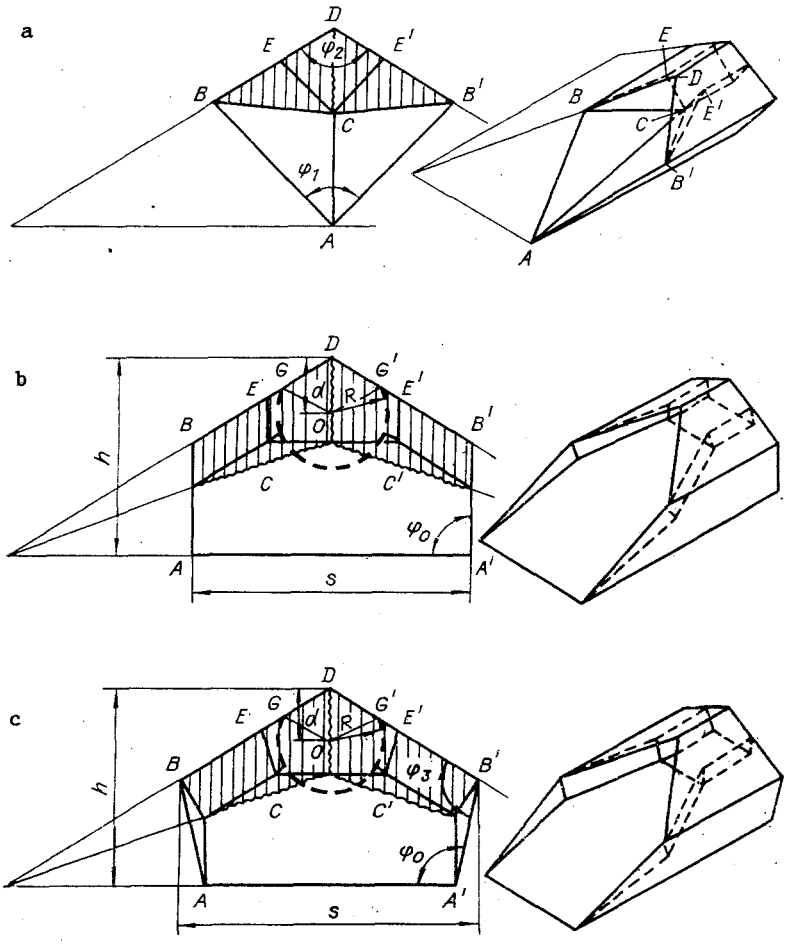

Fig. 3

TABLE 1

M_{ID}	ϑ_1^0	ϑ_2^0	$(\varphi_2/2)^0$	$\bar{F}_{input}$
2.5	9.1	14.3	58.2	1.93
4.0	9.7	13.7	55.3	3.16
8.0	10.5	18.3	61.3	8.34

is arbitrary. When $\varphi_1 = 180°$, we obtain the initial configuration (the simplified CAI in Fig. 1b), while for $\varphi_1 < 180°$, we have a sharp-nosed air intake configuration. The value of k for it is determined by the equation

$$k = [\operatorname{cosec}(\varphi_1/2) + \operatorname{cosec}(\varphi_2/2)]/\sqrt{\pi[\cot(\varphi_1/2) + \cot(\varphi_2/2)]}.$$

When $\varphi_1 = 90°$ and $\varphi_2 = 90$-$120°$, k = 1.12-1.15. This sectioning surface from the initial CAI (see Fig. 1c) can be thought of as an initial compression surface for the obtained CAI (Fig. 3a) – a V-shaped wing of ACBB', whose surface has a leading edge BAB', a break AC, and a trailing edge BCB'. The secondary discontinuities BCD and B'CD are generated here by secondary V-shaped asymmetric wings BECD and B'E'CD extending to the first. The gas dynamic parameters of the flow remain unchanged and coincide with the corresponding parameters for initial simple convergent flow. One should note that the CAI (see Fig. 1c) can be represented as a wedge with V-wings.

Simple cross sections, which differ from the initial planar compression surface, are obtained from the initial flow if one rounds off the sharp angles of the initial configuration (Figs. 3b, 3c), where the shapes of the cross sections for the captured stream and the channel input are similar and have pentagonal forms ABDB'A' and CEDE'C'. Here, k is found from Eq. (2), where

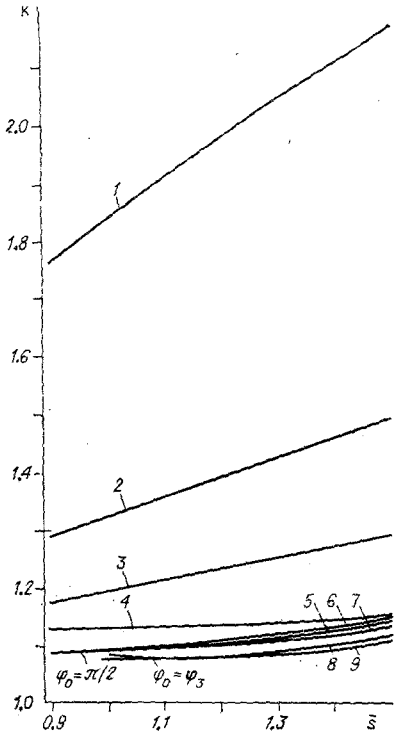

Fig. 4

$$P = h\{\bar{s} + \bar{s}\,\mathrm{cosec}(\varphi_2/2) + [2 - \bar{s}\cot(\varphi_2/2)](1 + \cos\varphi_0)\,\mathrm{cosec}\varphi_0\};$$
$$F = h^2\{4\bar{s} - \bar{s}^2\cot(\varphi_2/2) + (\cot\varphi_0)[2 - \bar{s}\cot(\varphi_2/2)]^2\}/4; \qquad (3)$$

$\bar{s} = s/h$; s is the width; and h is the height of the air intake (Figs. 3b, 3c).

Several geometric characteristics for a CAI are given in Table 1 that were determined according to the above method.

Values for the coefficient k as a function of the relative width of the cross section $\bar{s}$ for the CAI are given in Fig. 4 that were calculated by sectioning the initial flows (see Table 1). Hence, the group of closely positioned curves 5-7 (M_{ID} = 2.5; 4; 8) lie in the range of k = 1.09-1.15 and pertain to the channel cross section form with an angle of $\varphi_0 = \pi/2$ (Fig. 3b). For the group of curves 8 and 9 (M_{ID} = 4 and 8; k = 1.08-1.12), the form of the cross section is almost a regular pentagon ($\varphi_0 = \varphi_3$) (Fig. 3c). Since the transverse channel cross sections and the captured stream for these CAIs are similar, both groups of curves pertain to the cross sections and channel and to the captured stream.

It is evident from Fig. 4 that these CAI configurations have extremely compact channels. For a large range of relative cross section widths $\bar{s}$ from narrow ($\bar{s}$ = 0.9) to fairly wide ($\bar{s}$ = 1.2-1.4), the compactness is scarcely worse than the most compact figure – a circle (k = 1), but it is no greater than 10%. Hence, k is a weak function of $\bar{s}$.

For comparison, k as a function of $\bar{s}$ for a PAI is indicated in Fig. 4 (curves 1-4), which has the same degree of compression $\bar{F}_{input}$ as that for a comparable CAI for the same values of M_{ID} and ϑ_1. In contrast to a CAI for a planar air intake, the coefficient k for the cross section of the captured stream k_{ID} and the channel (the throat) k_T substantially differs. Values of k_T (curves 1-3) for the PAI are greater than those for a CAI and greatly increase with an increase in M_{ID} (curve 1 corresponds to M_{ID} = 8; 2 – 4.0; 3 – 2.5). This is because compression of the stream cross section in a PAI occurs only in a single direction and with an increase in the degree of compression $\bar{F}_{input}$ for an increase in M_{ID}. The substantial gain in a decrease in the area of the channel walls for the air intake obtained using the convergence principle is achieved at larger M_{ID}, i.e., for the flight velocities where it is especially important. The compactness of the cross section of the captured stream k_{ID} for a PAIs (curve 4) is better than that for their channels, which is also the case for the above CAIs.

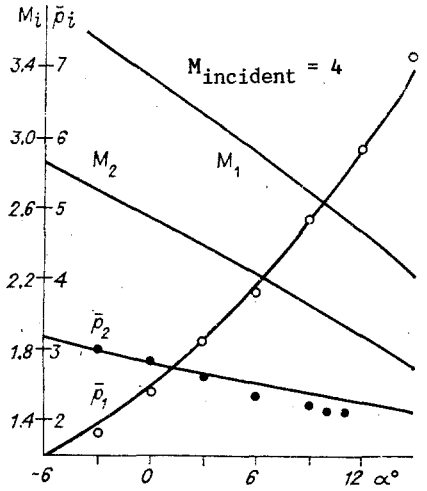

Fig. 5

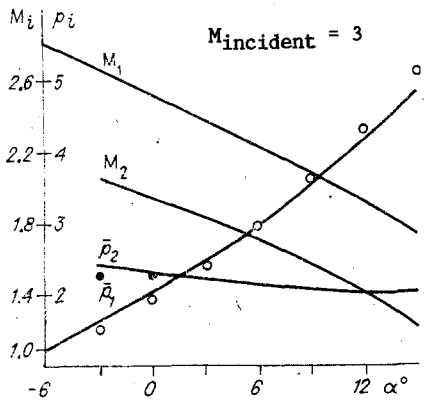

Fig. 6

The compactness of the CAI channel can be easily improved up to a limit, i.e., one can approximate the cross section of a circle (to obtain $k \approx 1$) almost without changing the geometry of the external compression section (Figs. 3b, 3c). Consequently, for $\angle GOG' = \varphi_2$ (the point O is the center of the circle), k is given by the equation

$$k = [\pi - (\varphi_2/2) + 1]/\sqrt{\pi[\pi - (\varphi_2/2) + \sin\varphi_2]}$$

and for $\varphi_2 = 90\text{-}100°$, $k \leq 1.02$.

The radius of the circle $R = \sqrt{F\cos\vartheta_1/\overline{F}_{input}[\pi - (\varphi_2/2) + \sin\varphi_2]}$, the distance from the vertex D of the angle φ_2 to the center of the circle $d = 2R\cos(\varphi_2/2)$, $\overline{F}_{input}$ and F are given by Eqs. (1) and (3).

For a PAI, however, similar attempts to obtain compact channel cross sections are complicated (as is evident, for example, from a comparison between Figs. 3b, 3c, and 1b), and the transition to the compact cross section takes up large sections of the channel length on the order of several calibers.

The compression flow in the external compression section for this class of CAI is three-dimensional in the design mode, but its parameters change only with a transition across planar shock waves and can be determined accurately and easily with known relations. For nondesign modes ($M_I \neq M_{ID}$, $\alpha \neq 0$), the flow parameters change only in the discontinuities but for different reasons, i.e., because of the outflow of the initial discontinuity from the leading edges and of the intersection above them. However, for the CAI configuration with the planar initial surface (see Figs. 3b, 3c) in nondesign modes, the flow remains planar or close to it in large regions. Therefore, one can use the same gas dynamic scheme as that for the design mode, i.e. the flow parameters change only with a transition across the shock waves, which are assumed to be planar. Only the angle of turn of the flow in the initial discontinuity must be determined as a sum of the initial wedge angle ϑ_1 and the angle of attack α. It is clear that this method of calculation is an approximation, and its accuracy will be worse if the parameters for the incident flow M_I and α greatly differ from the design values M_{ID} and $\alpha = 0$.

For a CAI configuration (see Fig. 3b) with $M_{ID} = 4$ and with the geometric parameters indicated in Table 1, results of making the approximation calculation for $M_I = 4$ and 3 over the range $\alpha = -6\text{-}15°$ are given in Figs. 5 and 6 in the form of dependences of M_i and $\overline{p}_i$ on α (M_i is the Mach number for the i-th discontinuity and $\overline{p}_i$ is the ratio of the pressures in the i-th discontinuity; i = 1-2); the small circles indicate data obtained from an experimental investigation of flow with the CAI model in [4, 5]. They agree with the calculated values. Thus, the approximation calculation method presented here can be used in some range of nondesign parameters for making estimates of CAI characteristics.

LITERATURE CITED

1. B. I. Gutov and V. V. Zatoloka, "Convergent input diffusors with an initial discontinuity and additional external compression," Aerofiz. Issled., Inst. Teor. Prikl. Mekh., Sib. Otd. Akad. Nauk, SSSR, No. 2 (1973).

2. B. I. Gutov and V. V. Zatoloka, "Spatial air intakes with external compression (convergent), constructed on the basis of planar flows," Aerofiz. Issled., Inst. Teor. Prikl. Mekh., Sib. Otd., Akad. Nauk, SSSR, No. 5 (1975).
3. B. I. Gutov and V. V. Zatoloka, "Example of numerical modeling for constructing convergent air intakes," ChMMSS, 10, No. 3 (1979).
4. B. I. Gutov and V. V. Zatoloka, "Calculation and experimental investigation of new configurations of convergent air intakes with spatial flow combinations," Preprint Inst. Teor. Prikl. Mekh., Sib. Otd., Akad. Nauk, SSSR, Nos. 30-83, Novosibirsk (1983).
5. B. I. Gutov and V. V. Zatoloka, "Experimental investigation of flow in a model of a convergent air intake with planar walls, Prikl. Mat. Teor. Fiz., No. 6 (1985).
6. G. I. Maikapar, "Wave resistance of nonaxially symmetric objects in a supersonic flow," Prikl. Mat. Mekh., 23, No. 2 (1959).
7. V. V. Keldysh and G. I. Maikapar, "Gas dynamic construction of supersonic jets," Izv. Akad. Nauk SSSR, Mekh. Zhidk. Gaza, No. 3 (1969).

AERODYNAMIC CHARACTERISTICS OF WAVE WINGS

A. I. Shvets

UDC 629.782.015.3+533.6.011.55

Optimal lifting forms are given much attention. We continue a study of traditional wings and of various new arrangements based on the conception of the wave wing — a Λ-wing with a planar shock wave on the leading edges. In analyses done on the basis of exact solutions, pyramidal nose ends with minimal resistance [1, 2] and a Λ-wing of minimal aerodynamic efficiency [3] were constructed. Calculations based on Newtonian theory [4] and experiments [5, 6] have established that the resistance of a star-shaped object at supersonic velocities is almost two times less than that for an equivalent cone, while the aerodynamic efficiency of Λ-wings exceeds the efficiency of an equivalent trangular wing by 10-15% [5, 7]. In our last study, we analyzed subsonic flow around of Λ-wings [8], the aerodynamic characteristics of a Λ-wing with a conical break on its surface [9] and with a break on the leading edge [10]. We will now give experimental results and a comparison of the aerodynamic efficiency of several types of wave wings: Λ-wings, triangular wings with a conical break, pryamidal objects with wings, and lined Λ-wings.

1. Λ-Wings. Models in the form of a combination of a thin central cone (with a half-angle of 7°) with two rigidly attached triangular wings have been tested (the angle of sweep in the plane of the wing is $\chi = 60°$). The obtained results indicate that a decrease in the included angle of the Λ-wing changes the buoyancy coefficient insignificantly, while the coefficient of head resistance is reduced. For a decrease in the angle Λ from 180 to 150°, the aerodynamic efficiency increases by 15-20% in comparison with the efficiency of a planar triangular wing. An increase in the efficiency of a Λ-shaped wing with a decrease in the included angle occurs not because of the increase in the buoyancy of the wing but due to the decrease in its resistance, i.e., an effect arises that greatly reduces the resistance of a body with a star-shaped cross section [6].

2. Conical Break of Triangular Wings. The effect of varying the cross section of a Λ-wing is schematically indicated in Fig. 1, where *a* is the original Λ-wing in the design mode with a planar shock wave; b and c denote the possible structures of the discontinuities for displacement of the internal fin from the leading edges and for formation of a convex angle in the plane of compression — there is a tendency for displacement of the shock wave inside the wing. For displacement of the internal fin to the leading edges — the formation of the concave angle — one approximates a fuselage positioned between the main planes of the wing with a system of shock waves displaced outwardly (Fig. 1d, e).

For a measurement of aerodynamic characteristics of wings with a break, four models have been tested simulating combinations of a thin central cone ($\theta = 7°$) and two rigidly attached

Moscow. Translated from Zhurnal Prikladnoi Mekhaniki i Tekhnicheskoi Fiziki, No. 2, pp. 62-68, March-April, 1987. Original article submitted February 28, 1986.

